4-17-2006

Early stages of soldering reactions

R A. Lord

Alexander Umantsev
Fayetteville State University, aumantsev@uncfsu.edu

Early stages of soldering reactions

R. A. Lord and A. Umantsev[a)]
Department of Natural Sciences, Fayetteville State University, 1200 Murchison Road, Fayetteville, North Carolina, 28301

(Received 14 February 2005; accepted 9 August 2005; published online 29 September 2005)

An experiment on the early stages of intermetallic compound layer growth during soldering and its theoretical analysis were conducted with the intent to study the controlling factors of the process. An experimental technique based on fast dipping and pulling of a copper coupon in liquid solder followed by optical microscopy allowed the authors to study the temporal behavior of the sample on a single micrograph. The technique should be of value for different areas of metallurgy because many experiments on crystallization may be described as the growth of a layer of intermediate phase. Comparison of the experimental results with the theoretical calculations allowed one to identify the kinetics of dissolution as the rate-controlling mechanism on the early stages and measure the kinetic coefficient of dissolution. A popular model of intermetallic compound layer structure coarsening is discussed. © *2005 American Institute of Physics*. [DOI: 10.1063/1.2058186]

I. INTRODUCTION

Soldering is a technological process of joining two base metals, substrates, through the use of a filler metal, solder, with a significantly lower melting point.[1] From the standpoint of Physical Metallurgy the crux of the soldering problem is the growth of intermetallic compounds (IMC's): Cu_6Sn_5, Cu_3Sn, Ni_3Sn_4, etc., between the solder and the substrate. The morphology of the compound layer depends strongly on the temperature of soldering: the growth of IMC's from solid-state diffusion couples gives a relatively planar layer of IMC.[2,3] Observations of the intermetallic growth in the solid-Cu(Ni)/liquid-Sn system (above the melting point of the solder) instead of a smooth layer always show rough compound layers, which is manifested in the appearance of scallops of the intermetallic phase.[4–9]

With time scallops grow larger but fewer, indicating that the coarsening process takes place.[6–8] The mechanism of coarsening is not fully understood yet. To describe this process Kim *et al.*[6] and Kim and Tu[10] suggested a two-flux nonconservative Ostwald ripening model, which is based on the assumption that "the rapid growth of the Cu_6Sn_5 compounds on the solder side can be explained by the dissolution of Cu into the liquid solder, precipitation, and the coarsening of the scallop-type Cu_6Sn_5 compound by Ostwald ripening" (p. 2339 in Ref. 6). Schaefer *et al.*[11] considered a problem of soldering with a saturated solder and introduced a model for the growth kinetics of IMC layer, which assumes that the grain-boundary diffusion is the predominant transport mechanism through the layer. The model also assumes that the IMC grains are approximately equiaxed at all times of the layer growth, which warrants coarsening of the structure. The drawback of the approach is that, although partially supported by experimental evidence (see Refs. 6 and 7), the assumption of equiaxed scallops renders unnecessary any discussion of a reason or driving force for coarsening.

Correct description of the IMC structure coarsening is not possible without a clear picture of the mechanism of scallop formation and growth. As it has been rightfully noted in Ref. 6: "…there is no report on why the interface" of IMC layer "appears scallop edge." Hayashi *et al.*[4] suggested that "the reason why Cu_6Sn_5 has a scallop-edge appearance is probably due to the fact that Cu_6Sn_5 dissolves faster along the grain boundary." However, the authors did not present a solid proof of that and did not attempt to study the dissolution rate quantitatively. Kawakatsu *et al.*[12] studied the growth of IMC's between solid plates of copper and liquid tin either pure or saturated with copper. They found that the time exponents of the thickening of Cu_6Sn_5 layer were significantly different in these cases: it was 0.38 in the case of saturated solder and 1 in the case of pure tin. Comparing these results with their early experiments with pure solder[13] they found that the IMC phase "grew in intensive competition with the dissolution of solid copper." Blair *et al.*[14] studied the dissolution of copper wires into molten tin and found that "there is evidence that the IMC grows into the solder matrix while still attached to a Cu substrate." Boettinger *et al.*[15] studied the effect of the thickness of Sn–Pb eutectic solders on the IMC growth and dissolution of copper. Nonreacting surface of copper was masked out by an inert Mo film, which preserved the orirnal surface as the reference plane. The authors found that the dynamics of IMC/solder boundary was nonmonotonic: the boundary moved in the direction of the substrate for some time that depended on the thickness of the solder before turning in the direction of the solder. The changeover was associated with the saturation of the solder. Recently, Ghosh[16] reported the results of a study of dissolution and interfacial reaction between Sn–3.0Ag–0.7Cu solder and the thin-film Ti/Ni/Ag metallization; Ma *et al.*[17] published a study of dissolution of a planar IMC Cu_6Sn_5 which was initially formed by solid-state aging with concomitant scallop formation during subsequent reflows. Unfortunately, rather complex multicomponent system in the former case and intricate reflow cycle in the latter case did not allow the authors to come to definite conclusions regarding the physical reason for undulations during the IMC layer formation.

[a)]Electronic mail: aumantsev@uncfsu.edu

A growing IMC layer is bound by two interfaces, with the substrate and solder. Due to the very low solubility and very slow diffusion of tin in solid copper the IMC/substrate interface should be moving in the direction of the substrate phase transforming it into the IMC phase. The situation on the IMC/solder boundary is much less obvious: requirements of mass balance and phase equilibrium allow the interface to move in the direction of the solder phase or in the opposite one. The experiments with inert markers in solid-state Cu–Sn diffusion couples[2] provide a definite answer to this question for solid solders: the IMC/solder boundary moves in the direction of the solder. The literature, unfortunately, does not provide a comparable resolution of the problem in the case of liquid solders. When the layer grows from the solder bath saturated with copper,[4,11] the simple mass balance requires the IMC/solder boundary to move in the direction of the solder because there are no concentration gradients in the latter. It is not so easy to determine the direction of motion of this boundary when the IMC layer grows from undersaturated or pure-tin solder. Lea[1] discussed this case in general terms of fluxes of species but did not come to definite conclusions. The assumption of "the rapid growth of the Cu_6Sn_5 compounds on the solder side…"[6] seems to be supported by the experimental evidence from the studies of wetting reaction between Cu substrate and molten eutectic Sn–Pb solder (Fig. 7 in Ref. 18 and Fig. 9 in Ref. 19). However, these micrographs reveal an IMC layer after soldering for a long time and do not shed light on the process of layer formation. There is extensive evidence in the literature on reactive wetting that when a molten drop of metal spreads on a metal substrate, it partially dissolves the substrate.[20,21] Liquid spreading experiments, however, provide examples of dissolution without visible IMC formation.

Theoretically the problem of intermetallic growth may be described within the framework of a multiphase Stefan problem.[22] Mei *et al.*[23] calculated the rate of motion of different interphase boundaries in a solid-solid diffusion couple and found that the IMC layer grows in both directions with respect to the initial position, which was consistent with the experiments in Ref. 2. This approach could have also been used for molten solders, at least on the early stages of IMC formation, because initial layers are almost flat. The approach of a Stefan problem, however, does not resolve the problem of the growth directions because of two reasons. Firstly, the answer is very sensitive to the diffusion coefficient in the IMC phase, which is not known independently. More importantly, many studies dismiss bulk diffusion as the rate-limiting process for the IMC layer growth from a solid/liquid couple largely on the grounds of the kinetics of thickening of the IMC phase: diffusion control yields the time exponent equal to $\frac{1}{2}$ while experiments give the numbers closer to $\frac{1}{3}$. We, however, do not find this argument totally convincing because in the literature one can find the whole spectrum of exponents from $1/5$ to $\frac{1}{2}$ depending on the temperature, time interval, and purity of solder.[4,5,12,15,24] In Sec. IV we will come back to the analysis of diffusion as a rate-controlling factor.

The main thrust of the present research is to establish the physical mechanism that controls the formation of an IMC layer from a solid-liquid couple and find the reason for the scallop-edge appearance of the layer. This problem may be solved by determining the characteristic growth mode of the IMC layer formation on the *early stages*, contrary to the experiments in Refs. 12 and 15. Specifically, the authors want to know what process is dominant on the molten-solder/IMC-layer boundary: is it the growth of IMC into the solder phase or the dissolution of the former by the latter? The other goals of the present research are to quantitatively study the dissolution of copper by molten solder and compare it with theoretical calculations.

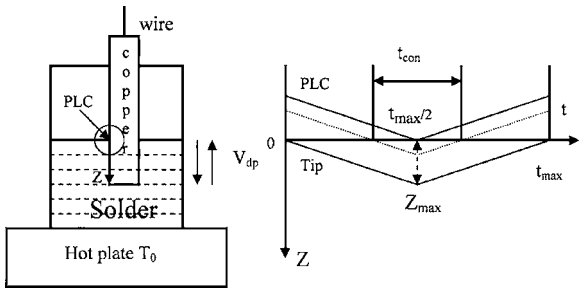

FIG. 1. Basic design of the experiment. T_0 is the temperature of the experiment, V_{dp} is the velocity of dipping and pulling out, PLC—point of the last contact, Z_{max} is the total length of the soldered part of the copper substrate, and t_{max} is the total time of contact between the two metals. The diagram on the right shows the position of the different points of the copper substrate—PLC, tip, and an arbitrary point in between—at different times of the experiment.

II. EXPERIMENT

A. Formulation of the experiment

The problem of the dominant process on the solder/IMC boundary will be resolved with the help of a pointed experiment, the main idea of which is to look at the early stages of IMC formation and determine the direction of the solder/IMC boundary motion. To do that the motion of the boundaries of the layer will be captured *relative to the original substrate/solder interface* when the incipient layer can be traced back to that interface, which will be called "the base line." In solid-state soldering reaction[2] the base line was designated by the inert markers. To establish the base line in a solid-liquid diffusion couple the authors in Ref. 15 used inert film on the nonreacting surface. We dipped solid copper samples into molten pure-tin baths and looked at the IMC layer in the vicinity of the line of the last contact between the substrate and the solder, which is the termination of soldering. In order to analyze the dynamics of IMC phase formation we choose the simplest possible system of pure molten tin on pure solid copper at constant temperature, in spite of the lack of technological applications for it. This technique should be of value for different areas of metallurgy because many experiments on crystallization may be described as the growth of a layer of intermediate phase between a molten phase of one composition and solid phase of another composition.

Figure 1 shows the basic design of the experiment. The copper substrates will be *dipped* into molten solder (pure tin) and *pulled out* in about 1 s at constant speed V_{dp} without any

"sitting time" in the solder. The microstructure will be analyzed around the line of the last contact. For microscopic observations the soldered sample will be cut perpendicular to this line, which exposes the point of last contact (PLC) on the cross section. Before and during the experiment copper and solder should be kept at the same temperature T_0.

As it has been stated in the Introduction, one of the goals of this project is to directly compare the experimental results of the soldering kinetics to its theoretical predictions, which usually take on the form of temporal relations. Dipping with constant speed will allow us to effectively transform the space axis Z along the base line into the time axis t of the soldering process (see diagram in Fig. 1) and measure the rate of growth or dissolution versus the time of contact between reacting metals at a specific point on the substrate:

$$t_{\mathrm{con}} = 2\frac{Z}{V_{\mathrm{dp}}}, \quad V_{\mathrm{dp}} = 2\frac{Z_{\max}}{t_{\max}}. \tag{1}$$

Here $Z_{\max}$ is the total length of the soldered part of the copper substrate and $t_{\max}$ is the total time of contact between the two metals. The factor "2" in Eq. (1) appears because each point on the copper surface will be traversed twice by the surface of the solder.

B. Implementation of the experiment

All metals for the experiments were provided by Kester Solder Corporation. Two different sources of copper were used: 25 μm layers of copper mounted on computer-grade fiberboard and rolled 0.5-mm-thick sheets of pure copper. Rolled copper was sectioned into small coupons approximately 2.5×2.5 mm^2. Copper coupons were placed between two pieces of straight-machined steel and pressed flat to remove contours from the surface of the coupons, sanded through four different (280, 360, 420, and 600) grits of silicon carbide sandpaper. Before the soldering, all samples were polished with a soft cloth and alumina surface polish starting at 6 μm and graduating through 1.0–0.3 μm. After polishing, all samples were rinsed in distilled water to remove any polish residue from the surface of the copper and suspended on copper wires. Usually the fiberboard-mounted copper had better surface and cleaner results. The use of pure copper coupons was to ensure that the entire sample of copper did not dissolve during the soldering process.

All samples were treated with a commercial-grade flux, which coated the surface of the polished samples suspended from copper wires and evaporated from the surface of the samples during heating. Different fluxes were used for experimental purposes. Kester rosin paste flux SP-44 provided soldered joints with fewer microvoids allowing better observation. All of the oxides and impurities on the surface of the molten tin were scraped off leaving a clean pure tin to dip the copper strips into. Optical investigations of the treated but unsoldered samples showed that the surface was free of oxides and had the standard deviation from a flat plane of 0.12 μm, which constitutes the main part of the experimental error of the interface position measurement.

Ceramic crucibles were used to melt the pure tin pellets. To avoid the effect of contamination of solder with copper, a separate bath of pure tin was used for each experiment. The melt was heated to specific temperatures T_0 between 250 and 350 °C at approximately 10° increments. At the same time copper samples were heated to a temperature $T_{\mathrm{Cu}}=T_0+\Delta T$ above that of the molten tin bath to compensate for heat loss during transfer of the sample from the hot plate to the tin bath. The temperature ΔT lost by copper samples between the hot plate and the bath was estimated in previous, independent trials for each experimental temperature T_0. Copper coupons were dipped in tin for desired maximum contact time (approximately 1 s) at a constant velocity without any sitting time, see Fig. 1, then pulled out from the tin bath and dipped into an ice-water bath to stop the IMC growth. The total "soldering time" of each point is

$$t_{\mathrm{sol}} = t_{\mathrm{col}} + t_{\mathrm{con}}(Z). \tag{2}$$

The time constant t_{col} of the sample transfer between the tin bath and ice-water brine was estimated as 0.5 s. More accurate estimate of this constant is not important because all parts of the soldered region get the same time shift. In Sec. IV experimental results of the kinetics of IMC growth will be analyzed versus the contact time. Experimental errors of the contact times came mainly from the measurements of $t_{\max}$ and constituted $\sim$1%. The shortcomings of Fig. 1 and Eq. (1) associated with the wetting properties of the solder are discussed in the Appendix A.

After the sample is pulled out of the solder, different amounts of tin stick to the substrate depending on the flux used and temperature of the experiment (more solder remains at lower temperatures). Once the procedure was completed the samples were cross sectioned with a diamond-tipped wafering blade, mounted in a low-temperature epoxy compound, and polished for microscopic observations using an inverted compound-light microscope Olympus-Tokyo with a polarized light source. No etching was used in preparation for microscopy, because etching is known to remove soft layers of solder and might distort the PLC. A digital video camera Fugi-HC-300Z was used to capture the images of the samples observed with the microscope. Digital photos were imported into ADOBE PHOTOSHOP. The images were rotated, cropped, and pieced together without changing the aspect ratio of each original photo, in order to make a panorama that represents a sample. Measurements taken by PHOTOSHOP were converted into the true metric measure of each picture based on the microscopic magnification. All of the results described below come from the optical observations of intermetallic structures in polarized light. Scanning electron microscope (SEM) study of selected samples was performed but did not bring new results (in addition to what already can be found in the literature) and, therefore, was not included in the present publication. One of the reasons why SEM did not produce interesting pictures was our choice not to etch the samples.

III. RESULTS OF THE EXPERIMENTS

Figure 2 represents typical micrographs of cross-sectioned samples that were soldered at different temperatures and for different time periods. Figure 2(a) shows the

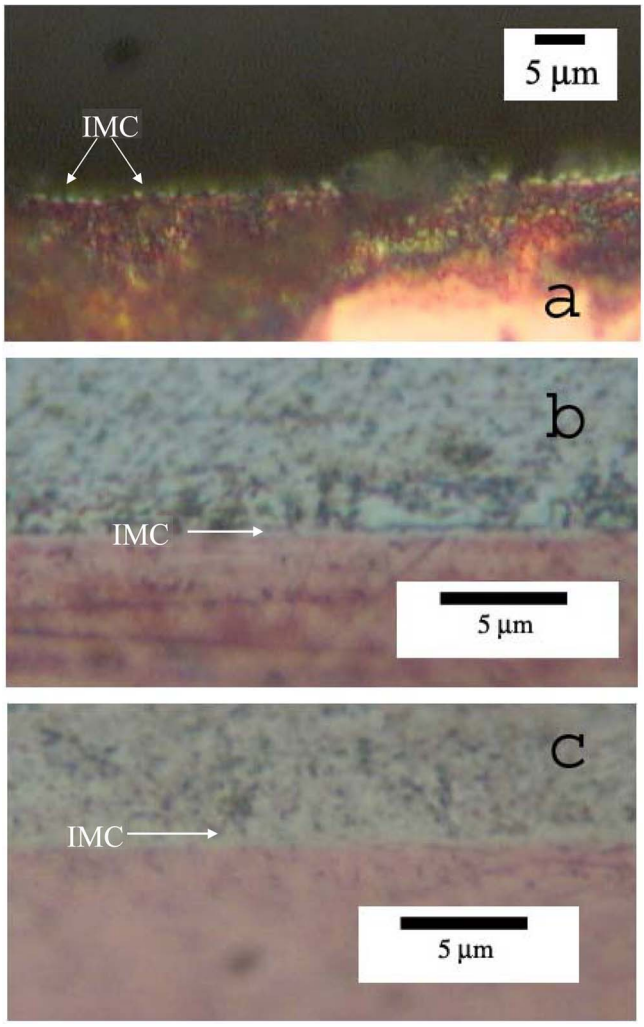

FIG. 2. (Color) Polarized light observations of the different sections of the samples soldered at different temperatures and for different time periods. Red—copper substrate; silvery—tin-based solder. (a) Close to PLC; $T_0=287\ ^\circ\mathrm{C}$; $t_{max}=9.61$ s. Individual nuclei of the IMC phase are visible on the substrate. (b) Middle of the soldered region; $T_0=253\ ^\circ\mathrm{C}$; $t_{max}=0.97$ s. Undulated IMC layer is visible in the middle. (c) End of the soldered region; $T_0=253\ ^\circ\mathrm{C}$; $t_{max}=0.97$ s. Undulated IMC layer has practically the same wavelength as in (b).

region very close to PLC where the first nuclei of IMC phase are discernable in the polarized light. The size of the first nuclei was 0.4–0.8 μm in diameter depending on the temperature of soldering. One can clearly see that even at the conception the individual nuclei (grains) are separated by the valleys approximately of the same size as the grains. Figure 2(b) depicts an undulated IMC layer from the middle section of the soldered region; the average thickness of the layer is $\sim$0.5 μm; the wavelength of undulations is $\sim$0.8 μm. In some cases, individual grains of the layer were separated by the channels, which were barely resolved by the optical microscope; their thickness was estimated as $\sim$0.2 μm. Figure 2(c) was taken from the end section of the soldered region of the same sample as in Fig. 2(b). The thickness of the layer is larger, but the wavelength of the undulations is practically the same. That is, no visible coarsening was observed at the early stages of IMC layer formation. No ε phase (Cu_3Sn) was visible at the optical magnification in the early stage of the transformation.

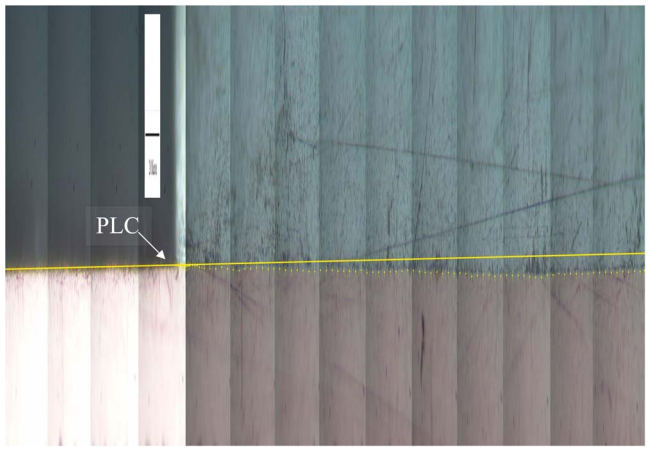

FIG. 3. (Color) Panoramic view of 14 cross-section micrographs of a sample that was soldered for 0.97 s at $T_0=253\ ^\circ\mathrm{C}$. The white bar in the upper left corner actually is a square with the side of 20 μm. The solid line is the base line, and the dotted line represents the position of the leading edge of the IMC phase.

To give the reader a better perspective of the experimental results 14–16 sections of the sample around PLC were assembled into a panoramic view and contracted tenfold in the horizontal Z direction for convenience of observations, see Fig. 3. PLC was clearly identifiable for most of the samples; in some cases, however, it was smeared by the wetting halo, size of which depended on the flux. Individual grains of IMC phase can be seen as close to the PLC as possible; a continuous layer of the compound, however, starts at a certain distance from this point. The base line was drawn such as to minimize the mean deviation from the surface points of the unprocessed part of the Cu substrate, i.e., the part which has never been in contact with the solder. These points can be seen left of PLC in Fig. 3.

IMC layer and even its first nuclei were always observed *below* the base line. This can be explained by the disparity of the diffusion coefficients in the melt and solid: as the solder gets in contact with the substrate, the process of mutual diffusion starts and atoms of Cu diffuse into molten tin while atoms of tin diffuse into solid Cu. However, Cu atoms in the melt will be diffusing away from the interface at much greater speed than Sn atoms in the solid due to the great difference of the diffusion coefficients. Therefore, the areas adjacent to the interface on the solder side will not be able to reach the required concentration of IMC, while on the substrate side the necessary concentration will be reached first and the nuclei will be conceived. Figure 3 also shows that the thickness of the IMC layer is much smaller than the depth of the dissolved substrate.

In Fig. 4 is sketched the early stage of the IMC (Cu_6Sn_5) layer formation process, which can be called the "creation-dissolution mechanism" (CDM). Indeed, the leading edge, IMC/substrate boundary, is moving in the direction of the substrate creating a new layer of the compound that consists of the grains of the IMC phase. At the same time, the trailing edge of the layer, solder/IMC boundary, is moving in the same direction with almost the same speed dissolving the newly formed grains of the compound. The small difference in the leading and trailing edge velocities entails the rate of

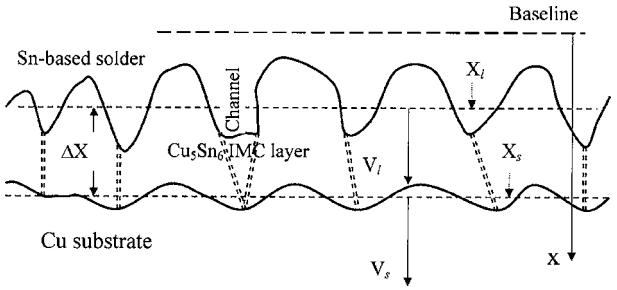

FIG. 4. Creation-dissolution mechanism of the Cu_6Sn_5 IMC layer growth. The thickness of the layer is not to scale with the thickness of the dissolved substrate. X_s is the average position of the leading edge, and X_l is the average position of the trailing edge. The speed of the leading edge V_s is just slightly greater than the speed of the trailing edge V_l. The double-dashed lines designate the grain boundaries.

growth of the IMC layer. The grain boundaries are dissolved faster than grains and will be replaced by the channels. In Fig. 4 X_s and V_s are the average depth (position below the baseline) and velocity of the leading edge, X_l and V_l are that of the trailing edge, while $\Delta X = X_s - X_l$ is the average thickness of the IMC layer.

In Fig. 5 we plot the depth X_s of the leading edge of IMC layer versus the contact time t_{con}, see Eq. (1), Fig. 1, and Appendix A. Three regions of different temporal behaviors can be identified on the plot: delayed, linear, and postlinear. These regions are represented in Figs. 2(a)–2(c), respectively. The slope of the linear part of the plot, $X_s(t_{con})$, is the speed of motion of the leading edge, V_s. In Table I the speed V_s of the linear region is shown for different temperatures and dipping/pulling-out speeds of the experiments. In the postlinear region motion of the leading edge slowed down dramatically or even receded back in some cases as in Fig. 5. The resolution of the optical microscope used for observations did not allow us to conduct a systematic study of the temporal dependence of the IMC layer thickness on the early stages, although that would have been desirable. In Table I we show only the layer thickness ΔX at the end of the soldering process, i.e., at $t_{con} = t_{max}$.

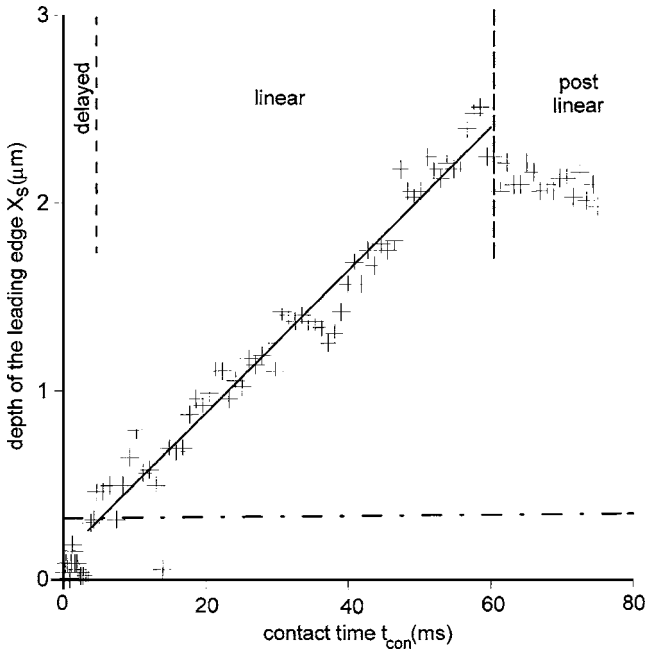

FIG. 5. Depth of the leading edge of the IMC layer X_s vs the contact time t_{con} for the sample in Fig. 3. Different regions: delayed, linear, and postlinear. The crosses represent the experimental points, the straight line is the linear fit on the linear stage, and the dash-dotted line represents the solution of the multiphase Stefan problem, Eq. (3).

IV. THEORETICAL ANALYSIS OF THE EXPERIMENTAL RESULTS

As we stated in the Introduction, the goal of the present research is to establish the physical mechanism that controls the formation of IMC phases during soldering. A materials science experiment can shed light on the physics of the mechanisms involved if the results of this experiment can be compared with the theory, describing the same process. In the case of IMC growth the theoretical constructs usually describe the temporal behavior of the system, which can be revealed experimentally through the series of observations of similar systems at different times. An advantage of the technique suggested in Sec. II is that it allowed us to capture the

TABLE I. Results of the experiment. Speed of dissolution V_s in the linear regime of transformation depending on the temperature of soldering T_0, maximum contact time t_{max}, and the speed of dipping/pulling-out V_{dp}. IMC layer thickness ΔX was estimated at t_{max}. C_l is the equilibrium solubility of copper in liquid tin at the temperature of the experiment (Ref. 27), μ is the kinematic viscosity of the fluid (Ref. 31), D_l is the interdiffusion coefficient in the solder (Ref. 26) k^* is an estimate of the kinetic coefficient of dissolution, and τ is the crossover time of switching from the kinetic to hydrodynamic regime of dissolution, Eq. (10).

Control parameters			Material parameters			Expt. results		Derived parameters	
T_0 (°C)	t_{max} (s)	V_{dp} (mm/s)	C_l (ml fr)	μ (mm^2/s)	D_l ($\mu m^2/s$)	$V_s+\Delta V$ (μm/s)	ΔX (μm)	k^* (mm/s ml fr)	τ (s)
253	0.97	8.87	0.022 10	0.2377	332.2	38±1	0.6	1.71	0.323
268	0.63	12.54	0.027 46	0.2178	371.1	36±2	0.5	1.30	0.518
276	1.03	11.41	0.030 31	0.2071	392.7	46±3	0.6	1.50	0.367
287	9.61	2.63	0.034 24	0.2041	423.3	15±1	0.9	0.447	4.09
304	0.60	16.67	0.040 31	0.2011	472.8	43±3	1.1	1.07	0.701
307	0.82	10.85	0.041 39	0.2002	481.8	63±2	0.7	1.52	0.345
334	0.64	15.47	0.051 03	0.1921	565.9	36±2	0.7	0.700	1.567
355	0.76	24.25	0.058 53	0.1858	635.4	65±3	1.1	1.11	0.599

entire IMC growth dynamics on a single photograph by relating the horizontal axis of the snapshot, Fig. 3, to the time axis of IMC growth and converting the set of spatial points into a time series, Fig. 5. This was achieved by dipping the sample at a constant rate and pulling it out at the same rate (Figs. 1 and 7). The position of the leading edge of IMC versus the soldering time, Fig. 5, reveals three different regions of the temporal behavior of the system: delayed, linear, and postlinear, which are also represented by Figs. 2(a)–2(c), respectively. The delayed region of Fig. 5 can be interpreted as the stage of nucleation of IMC grains, Fig. 2(a). The analysis of the $X_s(t_{\mathrm{con}})$ plots allowed us to estimate some of the parameters of nucleation: delay time as ~ 3 ms and the size of the first grains (nuclei) as $0.4-0.8$ μm in diameter.

After the nucleation of the IMC phase, a continuous layer of small grains of this phase forms between the substrate and the solder, Fig. 2(b); the growth of this layer proceeds by the CDM outlined in Fig. 4. One may ask a question: What physicometallurgical process controls this mechanism?

It has been explained in the Introduction that dissolution of the solid limited by the bulk diffusion and growth of IMC layer can be considered in the framework of a multiphase Stefan problem, which has been addressed in a number of publications.[22,23] Because the IMC layer is so thin, we will not discriminate below between X_l and X_s or between V_l and V_s. Instead, to characterize the dynamics of the layer we will use X and $V \equiv dX/dt$, which are $X_l < X < X_s$ and $V_l < V < V_s$. Applying the solution for the position of the boundary between the two phases[25] to the case of soldering from pure molten tin, where the interdiffusion coefficient in the solder, D_l, is much greater than that in the substrate and the equilibrium solubility of copper in liquid tin at the temperature of the experiment is $C_l \ll 1$, one can find that

$$X = 2C_l \sqrt{\frac{D_l t_{\mathrm{sol}}}{\pi}}. \tag{3}$$

Thus, the depth of the leading edge, Eq. (3), depends only on the known parameters, diffusion coefficient,[26] and solubility of copper in molten tin,[27] and can be compared with the experimental results directly, without any adjustable parameters. In Fig. 5 the dashed curve representing Eq. (3) turns out to be significantly below the experimental points. Hence, bulk diffusion in the solder is not potent enough to control CDM and should be ruled out as the dominant mechanism of IMC layer formation. On the early stages the layer is so thin that it is not a hindrance for its own growth. Hence, the internal processes, e.g., grain-boundary diffusion, cannot control the CDM either.

In recent publications,[17,28] the authors used a Nernst-Brunner approach to the kinetics of dissolution of solid A in liquid B. In the framework of this approach one assumes that the concentration in the liquid reaches the equilibrium solubility limit C_l on the boundary with solid, varies linearly in the diffusion boundary layer of constant thickness, and is uniform in the rest of the liquid due to intensive agitation. For the position of the front of dissolution, this yields

$$X = \frac{\Omega}{A}\left[1 - \exp\left(-\frac{KAt}{\Omega}\right)\right], \tag{4}$$

where K is the dissolution rate constant, A the area of the solid sample in contact with the liquid, and Ω the volume of the liquid. For a very large amount of solder, which is the case in our experiment, Eq. (4) yields $X = Kt_{\mathrm{con}}$ and constant rate of dissolution $V = K$ for all times. This contradicts the results of our experiment as the linear motion of the front was observed only during the very early stages and was replaced by the slow postlinear regime later, see Fig. 5.

The linear time dependence of $X(t_{\mathrm{con}})$ on the early stages replaced by a much slower postlinear regime may serve as a hint that the dominant mechanism of IMC layer formation is the nonequilibrium kinetics of dissolution when the rate of transformation is limited by the rate of separation of copper atoms from the solid substrate. The driving force for dissolution is the deviation of the concentration in the melt from its equilibrium value. In order to find the rate of dissolution one has to take into account that it does not occur uniformly and at once but rather proceeds in small increments at the interface between the phases. The principle most frequently invoked to determine the rate of transformation is the Onsager principle of linear response, which, in application to the present problem, states that the interfacial velocity is linearly proportional to the driving force of transformation. This principle proved to be valid in the cases of small driving forces exerted on the interfaces that possess certain degree of roughness. In Appendix B we outline the derivation of the relationship between the interfacial velocity and concentration in the melt c_X,

$$V = k(C_l - c_X). \tag{5}$$

Here k is called the compositional kinetic coefficient as opposed to the thermal one, which is used more often.[29]

On the early stages the concentration of copper in the solder immediately adjacent to the boundary can be estimated by assuming that the dissolved material spreads uniformly in a thin boundary layer, which contained no copper prior to the contact. Soldering process is always accompanied by convective flow of the solder induced by density differences of the substrate, solder, and IMC phase. In our experiments the convection flow was enhanced by the motion of the solid sample through the melt. As known, convective flow brings about momentum transfer and causes mixing in the boundary layer adjacent to the sample. The momentum transfer is the dominant process in the boundary layer, the thickness of which, $2\sqrt{(\mu t)}$, is determined by the kinematic viscosity of the fluid μ.[30,31] In t seconds the solder will dissolve (Vt) cubic centimeters of pure copper per square centimeter of the sample and spread it in the boundary layer. Hence, the concentration of copper in the layer will be

$$c_X = \frac{1}{2} V \sqrt{\frac{t}{\mu}}. \tag{6}$$

With time, changes of the concentration in the melt near the boundary, Eq. (6), cause changes of the interfacial velocity, Eq. (5). Then resolving Eqs. (5) and (6) one can find that

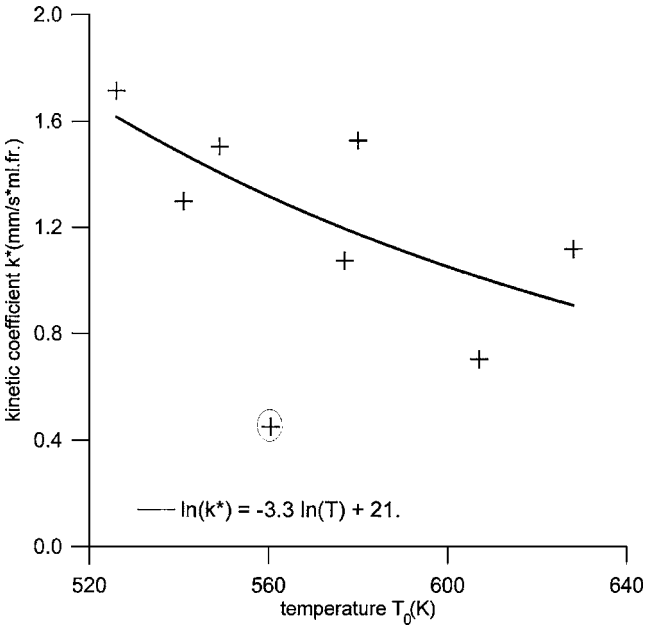

FIG. 6. Temperature dependence of the kinetic coefficient k^*. The circled value at $T_0=287\ ^\circ\mathrm{C}$ was not included into the fitting procedure.

$$V=\frac{kC_l}{1+(k/2)\sqrt{t/\mu}}. \tag{7}$$

Equation (7) shows that the initial stages proceed with constant speed, which corroborates the experimental observations expressed in Fig. 5. Significant slow down of the motion of the leading edge in the postlinear region may be explained by the transition from the kinetic to hydrodynamic regime of dissolution when diffusion of momentum becomes the rate-controlling factor.

Thus, the slope of the linear region of the plot $X(t_{\mathrm{con}})$ allows us to determine the kinetic coefficient of dissolution of copper in tin,

$$k^*=\frac{\mathrm{slope}X(t_{\mathrm{con}})}{C_l}. \tag{8}$$

The values of the kinetic coefficient k^* are plotted in Fig. 6 as a function of the absolute temperature $T_0(K)$ and fitted with a power-law equation,

$$k^*=\frac{B}{T^n}. \tag{9}$$

The best-fit values of the parameters in Eq. (9) were $n=3.3$ and $B=1.4\times10^9$; they may shed light on the physics of dissolution process, but this was not targeted in the present study.

The approach taken to derive Eq. (6) needs some clarification: it is valid only if the solder in contact with copper was fresh (pure tin) prior to the contact. As all the points of the copper coupon encompassed in Figs. 3 and 5 are near PLC, they were in contact with the solder for a short period of time around the instant $t_{\max}/2$ [see Eq. (1) and Fig. 1]. Hence, our approach is valid if around that time the average concentration in the boundary layer adjacent to PLC was much less than the solubility C_l; that is, the criterion of validity of this approach is

$$\frac{t_{\max}}{2}\ll\tau\equiv\frac{4\mu}{(k^*)^2}, \tag{10}$$

where τ is the characteristic time of the crossover from the purely kinetic to hydrodynamic regime of dissolution. Both k^* and τ are represented in Table I. Notice from Eq. (7) that this criterion also corresponds to the condition of constancy of V. As one can see from Table I, this criterion does not work well for most of the experiments. Hence, k^* can be used only as an estimate of the genuine kinetic coefficient k. Rather low value of k^* at $T=287\ ^\circ C$ can be explained by very long soldering time of this experiment ~10 s, compared to other experiments <1 s. That is why in Fig. 6 this value was omitted from fitting into Eq. (9).

V. DISCUSSION

In this section we will discuss some implications of the creation-dissolution mechanism of IMC layer formation (see Fig. 4). The mechanism manifests strong correlation between the moving boundaries of the layer. The formation of IMC occurs at the leading edge of the layer, IMC/copper boundary, through solid-state transformation. In the wake of the leading edge that moves into the substrate there will be left behind IMC grains separated by the grain boundaries. The trailing edge will be dissolving most of the just created IMC phase replacing the crystallites with melt and the grain boundaries with channels. The grain boundaries will be wetted by the solder and dissolved faster than the grains themselves, hence creating undulations of the layer, because grain boundaries are defects of crystalline structure. In this regard the authors agree with the conclusion made in Ref. 4 that not the equilibrium process of grain grooving but the fast dissolution of the grain boundaries is the primary cause of the formation of undulations of the layer in the form of scallops. CDM presents a reasonable proof of that despite the fact that our micrographs did not allow us to resolve the wetted boundaries.

As we have noted briefly in Sec. III, there was no coarsening of IMC phase observed on the early stages captured in the present study. However, the present study does not go far enough to make any conclusions regarding this process credible. Hayashi *et al.*[4] also conducted dipping experiments but for times much longer than in the present study and did not report any coarsening of the IMC structure.[32] Examination of the micrographs of the time sequences in Ref. 15 shows that coarsening started at different times depending on the thickness of the solder: the thicker the solder, the later it starts. Gagliano *et al.*[9] investigated the nucleation kinetics of IMC by hot dipping copper coupons in molten tin for 1 and 2 s at temperatures from 240 to 300 $^\circ C$. They found that between the first and second seconds of soldering the average crystallite size increased and the number of crystallites per unit area increased as well. Although the latter increase was very small, less than 20%, one may conclude that there was no coarsening observed in that experiment also. The small in-

crease in the number of crystallites per unit area may be explained by the dissolution of the scallops by the solder and the appearance of small grains on the surface.

Based on the similarities of the morphologies of IMC layers and mushy zones in solidification, Umantsev put forth a model of competitive growth of scallops as a mechanism of IMC structure coarsening. This model describes the coarsening of the secondary and primary branches of dendrites in solidification of alloys, which come into diffusional interaction with each other through the concentration or temperature field.[33] In the framework of the competitive growth model the driving force for coarsening would be the competition for the fresh, unprocessed Cu in the solder through overlapping concentration fields of the neighboring scallops. The mechanism of competitive growth for coarsening of IMC structure should be ruled out based on the creation-dissolution mechanism of the layer growth. Indeed, the competition between the scallops should develop only if they grow into the solder far from equilibrium, which is not the case here.

Analysis of the literature allows one to conjecture that coarsening of the IMC phase in tin/copper (nickel) systems starts only after the solder reaches its *saturation*. Assuming that dissolution proceeds very fast and is not a rate-limiting factor for diffusion in the solder, the characteristic time for saturation can be estimated as $C_l h^2/D_l$, where h is the thickness of the solder layer. This constitutes only 18 s for a 0.5 -mm-thick solder layer, which is much larger than in most of the studies where coarsening was observed. In the case of the experiments in Ref. 15 our conjecture is corroborated by the measurements of the position of the IMC/solder boundary, which changes the direction of motion around the solder saturation time. Then it makes perfect sense to assume that the surface energy reduction is the driving force of the IMC phase coarsening process, as the system is very near its equilibrium. This conclusion justifies the application of an Ostwald ripening model to the coarsening during soldering, as it was done in Refs. 6 and 10.

In many technological situations it is favorable to avoid coarsening of the IMC phase. On the basis of our analysis we can make a suggestion that in order to prevent IMC layer from coarsening one has to find means to avoid saturation of the solder. An obvious strategy is to use large amounts of solder, which may be difficult to implement technologically. There may be other, technologically more amenable, strategies to bypass saturation of the solder. However, if coarsening is desirable, than one should use saturated solders. Many of the remaining questions may be answered with the help of the numerical simulations of the IMC layer formation process which will be addressed in a following publication.

VI. CONCLUSIONS

On the basis of the analysis of the experimental results on the formation of IMC layer between a solid pure-copper substrate and molten pure-tin solder at different times and temperatures the following conclusions were made.

(1) The very first traces of the IMC phase appear in the form of individual nucleated grains separated by visible valleys. These grains grow and after as little as a few milliseconds merge to form a continuous undulated layer where the individual grains are separated by channels.
(2) The layer grows entirely on one side of the base line (original substrate/solder interface)—on the substrate side.
(3) The growth of the IMC layer from molten pure-Sn solder proceeds by the creation-dissolution mechanism—the leading edge of the IMC moves into the substrate and creates the compound while the trailing edge, moving in the same direction but slightly slower, dissolves the newly formed compound. The small difference in the leading and trailing edge velocities entails the rate of growth of the IMC layer.
(4) The initial stage of the growth of a continuous IMC layer is controlled by the kinetics of dissolution of the Cu substrate with the constant rate of transformation limited by the rate of separation of copper atoms from the solid substrate. This means that there is no local equilibrium on the boundaries of the layer with the original phases. The kinetic coefficient of dissolution of copper in pure tin is ~ 1 mm/s ml fr.
(5) The dissolution of the grain boundaries is the primary reason for the formation of undulations of the IMC layer in the form of scallops.
(6) Coarsening of IMC phase starts only when the solder reaches its saturation and the surface energy reduction is the primary driving force of the coarsening process. (This conclusion was made based on the analysis of the present study and literature.)

ACKNOWLEDGMENTS

The authors are grateful to Dr. M. Fine, Dr. G. Ghosh, and Dr. S. Vaynman of NU; Dr. J. Cahn, Dr. W. Boettinger, and Dr. K.W. Moon of NIST; and Dr. H. Conrad of NCSU for helpful discussions and the staff of the Department of Materials Science of NCSU for their help with the metallography. Metals were provided by Kester Solder Corporation (Des Plaines, IL). The work was supported by NSF Grant No. DMR-0244398 from the Material Theory program.

APPENDIX A: DYNAMIC WETTING

The diagram of Fig. 1 is an abstraction of the reality in the experiment. In the first place, the sharp corner on the trajectory $Z_{\text{tip}}(t)$ should be replaced with a smooth curve to avoid unphysical infinite acceleration. Trajectories of all other points on the sample are obtained by simple translation of $Z_{\text{tip}}(t)$ upward. In the second place, the surface of the solder does not remain flat and motionless during the experiment. When liquid solder gets in contact with the substrate the solder tends to form a meniscus due to the wetting properties of liquids. In static situation the meniscus would be formed by raising the contact line above the horizontal level of the surface of the melt. In our experiment, however, due to the fast motion of the sample, dynamics of the meniscus will be more complicated: it will be descending below the surface during the downward motion of the sample and will be rising

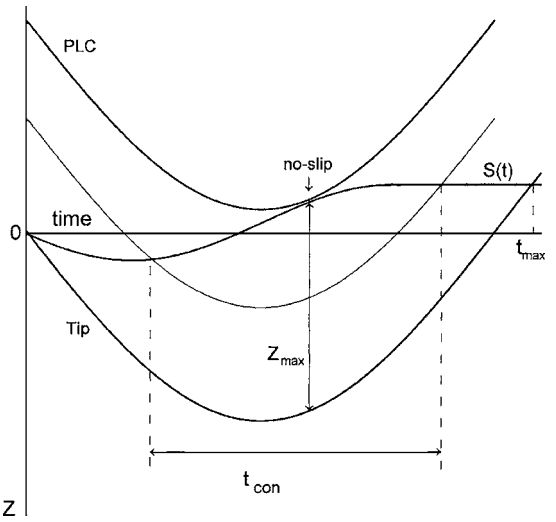

FIG. 7. Trajectories of the solder surface $S(t)$, the tip of the sample "tip," line of the last contact between the sample and solder "PLC," and an arbitrary point between tip and PLC.

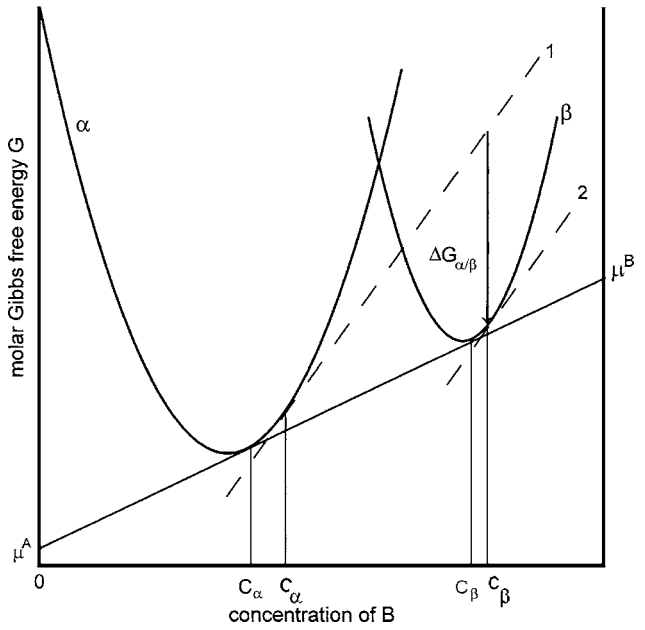

FIG. 8. Molar Gibbs free energy vs concentration diagram. α, initial; β, final phase; μ^A and μ^B—the chemical potentials of the corresponding species at equilibrium. Lines 1—the tangent line to the molar Gibbs free energy of phase α at the concentration c_α, and line 2—the tangent line to the molar Gibbs free energy of phase β at the concentration c_β.

above the surface when the sample is moving upward. Moon *et al.*[34] studied the dynamical aspects of the tin-based solder wetting and found that the maximum height of rise of the meniscus was $H_{\text{men}} \approx 1.8$ mm and the maximum speed $V_{\text{mem}} \approx 6.2$ mm/s (see Table V in Ref. 34). These data allow one to sketch on the diagram, Fig. 7, position of the solder contact line versus time, trajectory $S(t)$. Uneven depth of depression and height of rise of the meniscus is due to the resultant of the wetting, buoyancy, and viscous stress forces, which is directed upward. With the help of this trajectory one can find the position of the line of the last contact Z_{PLC} and the contact time t_{con} of any point on the copper sample. Z_{PLC} is the line where the condition of no slip is achieved on the upward swing of the experiment. To find it one has to translate the tip-trajectory upward until it is tangential to the solder surface trajectory $S(t)$. The vertical distance between Z_{PLC} and Z_{tip} gives $Z_{\max}$. The contact time t_{con} will be determined by the intersections of the respective $Z(t)$ trajectory with the solder surface trajectory $S(t)$. The soldering time and dipping/pulling-out speed still can be estimated by Eq. (1) if $Z_{\max} \gg H_{\text{men}}$ and $2Z_{\max}/t_{\max} \gg V_{\text{men}}$, which has been the case in the present experiment with the exception of one (at 287 °C) discussed in the paper. Also, in order to avoid significant influence of the reactive spreading effect, the speed of dipping V_{dp} must be significantly greater than the speed of the contact line spreading due to reactive wetting. The latter can be estimated from Fig. 5 in Ref. 21 as 10 μm/s.

APPENDIX B: KINETICS BOUNDARY CONDITION

The approach used here is very similar to that taken by Baker and Cahn[35] and Hillert[36] to derive the driving force for precipitation. However, our problem is different so as some of the assumptions used. All this justifies the inclusion of the derivation into the present paper.

Consider a transformation of a binary A-B alloy from the α phase at the concentration of B-species c_α into the β phase of the concentration c_β, see Fig. 8. In order to derive the condition on the boundary between the two phases that accounts for disequilibrium on it, we shall invoke the Onsager principle of linear response. In application to the present problem it means that

$$V = M\Delta G_{\alpha/\beta}. \tag{B1}$$

Here M is the interface mobility and $\Delta G_{\alpha/\beta}$ is the driving force for the formation of a small quantity of the minority phase β from a large quantity of the existing phase α or dissolution of the existing phase β in a large quantity of phase α. The first step in the process of formation is to bring together c_β particles of the α phase (proper concentration but improper phase content). The second step is to transform these particles into the final phase β. Obviously, the first step is the diffusion process, which is not of concern here. The driving force for the second step is

$$\Delta G_{\alpha/\beta} = G_\alpha(c_\beta/c_\alpha) - G_\beta(c_\beta). \tag{B2}$$

Here $G_\beta(c_\beta)$ is the molar Gibbs free energy of the β phase at the concentration c_β and $G_\alpha(c_\beta/c_\alpha)$ can be understood as the molar Gibbs free energy of c_β particles that are still in the α state at the concentration c_α. In the case of dissolution diffusion and transformation steps proceed in the reverse order; the driving force changes sign, which entails the change of the direction of motion of the interface.

The molar Gibbs free energies can be expressed through the appropriate chemical potentials $\mu_{\text{phase}}^{\text{species}}$:[35,36]

$$\begin{aligned} G_\beta(c_\beta) &= c_\beta \mu_\beta^B(c_\beta) + (1 - c_\beta)\mu_\beta^A(c_\beta), \\ G_\alpha(c_\beta/c_\alpha) &= c_\beta \mu_\alpha^B(c_\alpha) + (1 - c_\beta)\mu_\alpha^A(c_\alpha). \end{aligned} \tag{B3}$$

For the driving force, Eq. (B2), this yields

$$\Delta G_{\beta/\alpha} = c_\beta[\mu^B_\alpha(c_\alpha) - \mu^B_\beta(c_\beta)] + (1-c_\beta)[\mu^A_\alpha(c_\alpha) - \mu^A_\beta(c_\beta)]. \quad \text{(B4)}$$

Notice that this expression differs from Eq. (38) of Ref. 36 in that we do not imply c_β to be equal to its equilibrium value C_β.

Using the relations between the chemical potentials and molar Gibbs free energies,

$$\mu^A = G - c\frac{\partial G}{\partial c}, \quad \mu^B = G + (1-c)\frac{\partial G}{\partial c},$$

and the Gibbs-Duhem equation for a binary alloy

$$(1-c)\frac{\partial \mu^A}{\partial c} + c\frac{\partial \mu^B}{\partial c} = 0$$

one can obtain that

$$\frac{\partial \Delta G_{\beta/\alpha}}{\partial c_\beta} = \frac{\partial G_\alpha(c_\alpha)}{\partial c_\alpha} - \frac{\partial G_\beta(c_\beta)}{\partial c_\beta} \quad \text{(B5)}$$

and

$$\frac{\partial^2 \Delta G_{\beta/\alpha}}{\partial c_\beta^2} = -\frac{\partial^2 G_\beta(c_\beta)}{\partial c_\beta^2}. \quad \text{(B6)}$$

On the grounds of the thermodynamics of irreversible processes one may argue that, given the concentration of the phase α, c_α, the concentration of the phase β, c_β, must be such that *maximizes* the driving force. Then Eq. (B5) shows that the optimum driving force is achieved at the concentration of the phase β where the tangent slope of the molar Gibbs free energy (line 2 in Fig. 8) is equal to that of the phase α at the given concentration c_α (line 1 in Fig. 8);

$$\frac{\partial G_\alpha(c_\alpha)}{\partial c_\alpha} = \frac{\partial G_\beta(c_\beta)}{\partial c_\beta}. \quad \text{(B7)}$$

Equation (B6) shows that the driving force is at maximum if this concentration is not in the spinodal region that is, the phase β is stable.

If, at the temperature of transformation, the concentrations c_α and c_β are not far from their equilibrium values, C_α and C_β, then the free energies in Eq. (B7) can be expanded in a Taylor series and truncated at the second-order term. Using the condition of equal chemical potentials of species at equilibrium, the optimal concentration of the phase β will take the form

$$c_\beta = C_\beta + (c_\alpha - C_\alpha)\frac{G''_\alpha(C_\alpha)}{G''_\beta(C_\beta)}. \quad \text{(B8)}$$

For the distribution coefficient Eq. (B8) yields an expression

$$d = \bar{d} + \frac{(c_\alpha - C_\alpha)}{C_\alpha}\left[\frac{G''_\alpha(C_\alpha)}{G''_\beta(C_\beta)} - \frac{C_\beta}{C_\alpha}\right], \quad \text{(B9)}$$

where $\bar{d}$ is the distribution coefficient at equilibrium. Equation (B9) shows that our assumption of the maximum driving force does not allow for the solute trapping effect. This assumption can be used here because the solute trapping effect is not expected in the problem considered in the present paper.

Plugging Eq. (B8) into Eq. (B4) one can find the expression for the optimal driving force of the transformation,

$$\Delta G_{\beta/\alpha} = (c_\alpha - C_\alpha)(C_\beta - C_\alpha)G''_\alpha(C_\alpha). \quad \text{(B10)}$$

For the kinetic boundary condition, Eq. (B1), this yields

$$V = k(c_\alpha - C_\alpha), \quad k = M(C_\beta - C_\alpha)G''_\alpha(C_\alpha). \quad \text{(B11)}$$

As one can see from Eq. (B11), the driving force for the interface motion is the deviation from equilibrium in the majority phase α. Details of the thermodynamics of the minority phase β are "hidden" in the kinetic coefficient k. That is why we can use Eq. (B11) in a more complicated case of three phases if the thickness of the intermediate phase is small. The relationship, Eq. (B11), can be used as a boundary condition that replaces the equilibrium one for the solution of a long-time dissolution problem. Notice that in the case of dissolution $c_\alpha < C_\alpha < C_\beta$, which yields $V < 0$.

[1] C. Lea, *A Scientific Guide to Surface Mount Technology* (Electrochemical Publications, Ayr, Scotland, 1988), p. 309.
[2] M. Onishi and H. Fujibuchi, Trans. Jpn. Inst. Met. **16**, 539 (1975).
[3] P. T. Vianco, K. L. Erickson, and P. L. Hopkins, J. Electron. Mater. **23**, 721 (1994); A. J. Sunwoo, J. W. Morris, Jr., and G. K. Lucey, Jr., Metall. Trans. A **23A**, 1323 (1992).
[4] A. Hayashi, C. R. Kao, and Y. A. Chang, Scr. Mater. **37**, 393 (1997).
[5] S. Bader, W. Gust, and H. Hieber, Acta Metall. Mater. **43**, 329 (1995).
[6] H. K. Kim, H. K. Liou, and K. N. Tu, Appl. Phys. Lett. **66**, 2337 (1995).
[7] G. Ghosh, J. Appl. Phys. **88**, 6887 (2000).
[8] R. A. Gagliano and M. E. Fine, JOM **53**, 33 (2001).
[9] R. A. Gagliano, G. Ghosh, and M. E. Fine, J. Electron. Mater. **31**, 1195 (2002).
[10] H. K. Kim and K. N. Tu, Phys. Rev. B **53**, 1 (1996).
[11] M. Schaefer, R. A. Fournelle, and J. Liang, J. Electron. Mater. **27**, 1167 (1998).
[12] I. Kawakatsu, T. Osawa, and H. Yamaguchi, J. Jpn. Inst. Met. **34**, 539 (1970).
[13] I. Kawakatsu and H. Yamaguchi, J. Jpn. Inst. Met. **31**, 1387 (1967).
[14] H. D. Blair, T.-Y. Pan, R. P. Cooper, J. M. Nicholson, R. H. Poulson, S. C. Stine, K. Ezis, and D. Miltin, Proceedings of the NEPCON West '94, Anaheim, CA, 27 February–4 March 1994 (unpublished), p. 543.
[15] W. J. Boettinger, K.-W. Moon, and C. A. Handwerker, Fall ASM/TMS Meeting, Cincinnati, OH, 1 November 1999 (unpublished).
[16] G. Ghosh, Acta Mater. **49**, 2609 (2001).
[17] D. Ma, W. D. Wang, and S. K. Lahiri, J. Appl. Phys. **91**, 3312 (2002).
[18] X. H. Wang and H. Conrad, Metall. Mater. Trans. A **26A**, 459 (1994).
[19] A. S. Zuruzi, C.-H. Chiu, S. K. Lahiri, and K. M. Chua, J. Electron. Mater. **28**, 1224 (1999).
[20] W. J. Boettinger, C. A. Handwerker, and U. R. Kattner, in *The Mechanics of Solder Alloy Wetting & Spreading*, edited by D. R. Frear, F. G. Yost, and F. M. Hosking (The Minerals, Metals, and Materials Society, Warrendale, PA, 1993).
[21] J. A. Warren, W. J. Boettinger, and A. R. Roosen, Acta Mater. **46**, 3247 (1998).
[22] J. S. Kirkaldy, Can. J. Phys. **36**, 917 (1958); W. Jost, *Diffusion in Solids, Liquids, Gases* (Academic, New York, NY, 1952) pp. 68–75; G. B. Gibbs, J. Nucl. Mater. **20**, 303 (1966); W. Seith and T. Heumann, in *Diffusion of Metals: Exchange Reactions* (Springer, Berlin, 1955); C. Wagner, Acta Metall. **17**, 99 (1969); L. I. Rubinstein, *The Stefan Problem* (AMS, Providence, RI, 1971), pp. 141–189; B. Ya. Lyubov, *Kinetic Theory of Phase Transformations* (National Bureau of Standards, Gaithersburg, MD, 1978), pp. 88–94.
[23] Z. Mei, A. J. Sunwoo, and J. W. Morris, Jr., Metall. Trans. A **23A**, 857 (1992).
[24] R. A. Gagliano and M. E. Fine, J. Electron. Mater. **32**, 1441 (2003).
[25] H. S. Carslaw and J. C. Jaeger, *Conduction of Heat in Solids*, 2nd ed. (Oxford University Press, Oxford, 1959), pp. 282–296; J. Crank, *The Mathematics of Diffusion* (Oxford University Press, Oxford, 1975), pp. 286–325.
[26] C. H. Ma and R. A. Swalin, Acta Metall. **8**, 388 (1960).
[27] Data from Thermocalc© Database were provided by G. Ghosh.

[28]V. I. Dybkov, *Growth of Chemical Compound Layers* (Cambridge International, Cambridge, UK, 1998), p. 135; S. Chada, W. Laub, R. A. Fournelle, and D. Shangguan, J. Electron. Mater. **28**, 1194 (1999); **29**, 1214 (2000).
[29]J. W. Christian, *The Theory of Phase Transformations in Metals and Alloys* (Pergamon, New York, 1965), p. 479; A. N. Ahmad, A. A. Wheeler, W. J. Boettinger, and G. B. McFadden, Phys. Rev. E **58**, 3436 (1998); J. J. Hoyt, M. Asta, and A. Karma, Mater. Sci. Eng., R. **41**, 121 (2003).
[30]H. Schlichting, *Boundary Layer Theory* (McGraw-Hill, New York, 1955), Chap. 12.
[31]*CRC Handbook of Physics and Chemistry* (CRC, Boca Raton, FL, 2004).
[32]Because Ref. 4 did not provide a time series of the soldering structures conclusion of no coarsening in that experiment was made on the basis of comparison with soldering structures at the same temperature from other publications.
[33]S.-C. Huang and M. E. Glicksman, Acta Metall. **29**, 717 (1981); A. Umantsev, V. Vinogradov, and V. Borisov, Sov. Phys. Crystallogr. **31**, 569 (1986).
[34]K.-W. Moon, W. J. Boettinger, M. E. Williams, D. Josell, B. T. Murray, W. C. Carter, and C. A. Handwerker, ASME J. Electron. Packag. **118**, 174 (1996).
[35]J. C. Baker and J. W. Cahn, *Solidification* (ASM, Metals Park, OH, 1971), pp. 23–58.
[36]M. Hillert, in *Lectures on the Theory of Phase Transformations*, edited by H. I. Aaronson (AIM, New York, NY, 1986).